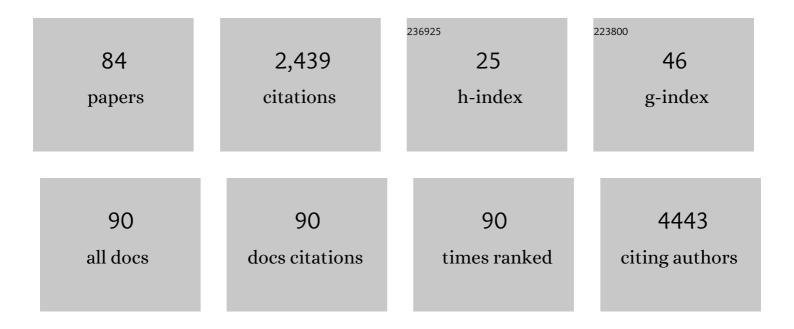
Michael Ingrisch

List of Publications by Year in descending order

Source: https://exaly.com/author-pdf/7309210/publications.pdf Version: 2024-02-01



#	Article	IF	CITATIONS
1	Artificial Intelligence in Chest Radiography Reporting Accuracy. Investigative Radiology, 2022, 57, 90-98.	6.2	16
2	Prognostic value of baseline imaging and clinical features in patients with advanced hepatocellular carcinoma. British Journal of Cancer, 2022, 126, 211-218.	6.4	18
3	Deep learning in CT colonography: differentiating premalignant from benign colorectal polyps. European Radiology, 2022, 32, 4749-4759.	4.5	12
4	Differential Spatial Distribution of TSPO or Amino Acid PET Signal and MRI Contrast Enhancement in Gliomas. Cancers, 2022, 14, 53.	3.7	12
5	Availability of Interventional Oncology in Germany in the Years 2018 and 2019 – Results from a Nationwide Database (DeGIR Registry Data). RoFo Fortschritte Auf Dem Gebiet Der Rontgenstrahlen Und Der Bildgebenden Verfahren, 2022, 194, 755-761.	1.3	1
6	REDUCE – Indication catalogue based ordering of chest radiographs in intensive care units. Journal of Critical Care, 2022, 69, 154016.	2.2	1
7	Sequential Organ Failure Assessment Outperforms Quantitative Chest CT Imaging Parameters for Mortality Prediction in COVID-19 ARDS. Diagnostics, 2022, 12, 10.	2.6	4
8	Tuning the Synergistic Interplay between Clinical MRI Contrast Agents and MR-Active Metal–Organic Framework Nanoparticles. Chemistry of Materials, 2022, 34, 3862-3871.	6.7	6
9	End-to-End Deep Learning Approach for Perfusion Data: A Proof-of-Concept Study to Classify Core Volume in Stroke CT. Diagnostics, 2022, 12, 1142.	2.6	2
10	Artificial intelligence assistance improves reporting efficiency of thoracic aortic aneurysm CT follow-up. European Journal of Radiology, 2021, 134, 109424.	2.6	25
11	Pneumothorax detection in chest radiographs: optimizing artificial intelligence system for accuracy and confounding bias reduction using in-image annotations in algorithm training. European Radiology, 2021, 31, 7888-7900.	4.5	14
12	Sources of systematic error in DCEâ€MRI estimation of lowâ€level bloodâ€brain barrier leakage. Magnetic Resonance in Medicine, 2021, 86, 1888-1903.	3.0	21
13	Machine Learning–based Differentiation of Benign and Premalignant Colorectal Polyps Detected with CT Colonography in an Asymptomatic Screening Population: A Proof-of-Concept Study. Radiology, 2021, 299, 326-335.	7.3	30
14	Risk Stratification for ECMO Requirement in COVID-19 ICU Patients Using Quantitative Imaging Features in CT Scans on Admission. Diagnostics, 2021, 11, 1029.	2.6	7
15	Reduction of missed thoracic findings in emergency whole-body computed tomography using artificial intelligence assistance. Quantitative Imaging in Medicine and Surgery, 2021, 11, 2486-2498.	2.0	11
16	Quantitative Analysis of the Time–Intensity Curve of Contrast-Enhanced Ultrasound of the Liver: Differentiation of Benign and Malignant Liver Lesions. Diagnostics, 2021, 11, 1244.	2.6	5
17	Bi-Centric Independent Validation of Outcome Prediction after Radioembolization of Primary and Secondary Liver Cancer. Journal of Clinical Medicine, 2021, 10, 3668.	2.4	1
18	Reproducibility of CT-Based Hepatocellular Carcinoma Radiomic Features across Different Contrast Imaging Phases: A Proof of Concept on SORAMIC Trial Data. Cancers, 2021, 13, 4638.	3.7	8

#	Article	IF	CITATIONS
19	Imaging neurovascular, endothelial and structural integrity in preparation to treat small vessel diseases. The INVESTIGATE-SVDs study protocol. Part of the SVDs@Target project. Cerebral Circulation - Cognition and Behavior, 2021, 2, 100020.	0.9	8
20	Outcome and Safety after 103 Radioembolizations with Yttrium-90 Resin Microspheres in 73 Patients with Unresectable Intrahepatic Cholangiocarcinoma—An Evaluation of Predictors. Cancers, 2021, 13, 5399.	3.7	17
21	Rheumatoid cervical pannus: feasibility of volume and perfusion quantification using dynamic contrast enhanced time resolved MRI. Acta Radiologica, 2020, 61, 227-235.	1.1	2
22	Joint Imaging Platform for Federated Clinical Data Analytics. JCO Clinical Cancer Informatics, 2020, 4, 1027-1038.	2.1	39
23	Single-center study: dynamic contrast-enhanced ultrasound in the diagnostic assessment of carotid body tumors. Quantitative Imaging in Medicine and Surgery, 2020, 10, 1739-1747.	2.0	6
24	Prognostic Value of Admission Chest CT Findings for Invasive Ventilation Therapy in COVID-19 Pneumonia. Diagnostics, 2020, 10, 1108.	2.6	8
25	Impact of Confounding Thoracic Tubes and Pleural Dehiscence Extent on Artificial Intelligence Pneumothorax Detection in Chest Radiographs. Investigative Radiology, 2020, 55, 792-798.	6.2	23
26	Multiparametric ultrasonographic analysis of testicular tumors: a single-center experience in a collective of 49 patients. Scandinavian Journal of Urology, 2020, 54, 241-247.	1.0	9
27	Availability of Transcatheter Vessel Occlusion Performed by Interventional Radiologists to Treat Bleeding in Germany in the Years 2016 and 2017 – An Analysis of the DeGIR Registry Data. RoFo Fortschritte Auf Dem Gebiet Der Rontgenstrahlen Und Der Bildgebenden Verfahren, 2020, 192, 952-960.	1.3	5
28	Artificial Intelligence Algorithm Detecting Lung Infection in Supine Chest Radiographs of Critically III Patients With a Diagnostic Accuracy Similar to Board-Certified Radiologists. Critical Care Medicine, 2020, 48, e574-e583.	0.9	25
29	Bayesian pharmacokinetic modeling of dynamic contrast-enhanced magnetic resonance imaging: validation and application. Physics in Medicine and Biology, 2019, 64, 18NT02.	3.0	6
30	MITK-ModelFit: A generic open-source framework for model fits and their exploration in medical imaging – design, implementation and application on the example of DCE-MRI. BMC Bioinformatics, 2019, 20, 31.	2.6	21
31	Digital Analysis in Breast Imaging. Breast Care, 2019, 14, 142-150.	1.4	2
32	Quantifying bloodâ€brain barrier leakage in small vessel disease: Review and consensus recommendations. Alzheimer's and Dementia, 2019, 15, 840-858.	0.8	134
33	Harmonizing brain magnetic resonance imaging methods for vascular contributions to neurodegeneration. Alzheimer's and Dementia: Diagnosis, Assessment and Disease Monitoring, 2019, 11, 191-204.	2.4	65
34	Radiation dose and image quality of high-pitch emergency abdominal CT in obese patients using third-generation dual-source CT (DSCT). Scientific Reports, 2019, 9, 15877.	3.3	5
35	Contrast enhancement is a prognostic factor in IDH1/2 mutant, but not in wild-type WHO grade II/III glioma as confirmed by machine learning. European Journal of Cancer, 2019, 107, 15-27.	2.8	30
36	Prediction of ⁹⁰ Y Radioembolization Outcome from Pretherapeutic Factors with Random Survival Forests. Journal of Nuclear Medicine, 2018, 59, 769-773.	5.0	27

MICHAEL INGRISCH

#	Article	IF	CITATIONS
37	Feasibility and robustness of dynamic 18F-FET PET based tracer kinetic models applied to patients with recurrent high-grade glioma prior to carbon ion irradiation. Scientific Reports, 2018, 8, 14760.	3.3	15
38	Contrast enhancement as a prognostic factor in IDH1/2 mutant glioma Journal of Clinical Oncology, 2018, 36, 2029-2029.	1.6	0
39	Pre-therapeutic factors for predicting survival after radioembolization: a single-center experience in 389 patients. European Journal of Nuclear Medicine and Molecular Imaging, 2017, 44, 1185-1193.	6.4	25
40	Technical Note: Quantitative dynamic contrast-enhanced MRI of a 3-dimensional artificial capillary network. Medical Physics, 2017, 44, 1462-1469.	3.0	2
41	Radiomic Analysis Reveals Prognostic Information in T1-Weighted Baseline Magnetic Resonance Imaging in Patients With Glioblastoma. Investigative Radiology, 2017, 52, 360-366.	6.2	96
42	Dynamic Contrast-Enhanced Magnetic Resonance Imaging Suggests Normal Perfusion in Normal-Appearing White Matter in Multiple Sclerosis. Investigative Radiology, 2017, 52, 135-141.	6.2	17
43	Dual energy CT allows for improved characterization of response to antiangiogenic treatment in patients with metastatic renal cell cancer. European Radiology, 2017, 27, 2532-2537.	4.5	48
44	Subclinical Disease Burden as Assessed by Whole-Body MRI in Subjects With Prediabetes, Subjects With Diabetes, and Normal Control Subjects From the General Population: The KORA-MRI Study. Diabetes, 2017, 66, 158-169.	0.6	102
45	Impact of fitting algorithms on errors of parameter estimates in dynamic contrast-enhanced MRI. Physics in Medicine and Biology, 2017, 62, 9322-9340.	3.0	9
46	Contrast-Enhanced Ultrasound with VEGFR2-Targeted Microbubbles for Monitoring Regorafenib Therapy Effects in Experimental Colorectal Adenocarcinomas in Rats with DCE-MRI and Immunohistochemical Validation. PLoS ONE, 2017, 12, e0169323.	2.5	23
47	EGFR-targeted nonviral NIS gene transfer for bioimaging and therapy of disseminated colon cancer metastases. Oncotarget, 2017, 8, 92195-92208.	1.8	18
48	Intravoxel Incoherent Motion Magnetic Resonance Imaging in Partially Nephrectomized Kidneys. Investigative Radiology, 2016, 51, 323-330.	6.2	18
49	Hypoxia-targeted 1311 therapy of hepatocellular cancer after systemic mesenchymal stem cell-mediated sodium iodide symporter gene delivery. Oncotarget, 2016, 7, 54795-54810.	1.8	31
50	Detection of pulmonary embolism with free-breathing dynamic contrast-enhanced MRI. Journal of Magnetic Resonance Imaging, 2016, 43, 887-893.	3.4	11
51	Imparting Functionality to MOF Nanoparticles by External Surface Selective Covalent Attachment of Polymers. Chemistry of Materials, 2016, 28, 3318-3326.	6.7	218
52	Surrogate MRI markers for hyperthermia-induced release of doxorubicin from thermosensitive liposomes in tumors. Journal of Controlled Release, 2016, 237, 138-146.	9.9	40
53	Evaluation of multimodality imaging using image fusion with MRI and CEUS in an experimental animal model. Clinical Hemorheology and Microcirculation, 2015, 61, 143-150.	1.7	3
54	Tracer kinetic modeling in myocardial perfusion quantification using MRI. Magnetic Resonance in Medicine, 2015, 73, 1206-1215.	3.0	12

MICHAEL INGRISCH

#	Article	IF	CITATIONS
55	Ex Vivo Perfusion-Simulation Measurements of Microbubbles as a Scattering Contrast Agent for Grating-Based X-Ray Dark-Field Imaging. PLoS ONE, 2015, 10, e0129512.	2.5	13
56	Reducing tumor growth and angiogenesis using a triple therapy measured with Contrast-enhanced ultrasound (CEUS). BMC Cancer, 2015, 15, 373.	2.6	7
57	DCE-MRI biomarkers for monitoring an anti-angiogenic triple combination therapy in experimental hypopharynx carcinoma xenografts with immunohistochemical validation. Acta Radiologica, 2015, 56, 294-303.	1.1	9
58	Resting-state networks in healthy adult subjects: a comparison between a 32-element and an 8-element phased array head coil at 3.0 Tesla. Acta Radiologica, 2015, 56, 605-613.	1.1	11
59	Dynamic Contrast-Enhanced Magnetic Resonance Imaging Measurements in Renal Cell Carcinoma. Investigative Radiology, 2015, 50, 57-66.	6.2	29
60	Correlation of Perfusion MRI and 18F-FDG PET Imaging Biomarkers for Monitoring Regorafenib Therapy in Experimental Colon Carcinomas with Immunohistochemical Validation. PLoS ONE, 2015, 10, e0115543.	2.5	6
61	Monitoring parotid gland tumors with a new perfusion software for contrast-enhanced ultrasound. Clinical Hemorheology and Microcirculation, 2014, 58, 261-269.	1.7	15
62	Evaluation of multimodality imaging using image fusion with ultrasound tissue elasticity imaging in an experimental animal model. Clinical Hemorheology and Microcirculation, 2014, 57, 101-110.	1.7	1
63	Assessment of Pulmonary Perfusion With Breath-Hold and Free-Breathing Dynamic Contrast-Enhanced Magnetic Resonance Imaging. Investigative Radiology, 2014, 49, 382-389.	6.2	26
64	Dynamic Contrast-Enhanced Magnetic Resonance Imaging Assessment of Kidney Function and Renal Masses. Investigative Radiology, 2014, 49, 720-727.	6.2	14
65	Evaluation of Neuroendocrine Liver Metastases. Investigative Radiology, 2014, 49, 7-14.	6.2	27
66	Tracer-kinetic modeling of dynamic contrast-enhanced MRI and CT: a primer. Journal of Pharmacokinetics and Pharmacodynamics, 2013, 40, 281-300.	1.8	93
67	Microbubbles as a scattering contrast agent for grating-based x-ray dark-field imaging. Physics in Medicine and Biology, 2013, 58, N37-N46.	3.0	39
68	Quantification of Pulmonary Perfusion with Free-Breathing Dynamic Contrast-Enhanced MRI – A Pilot Study in Healthy Volunteers. RoFo Fortschritte Auf Dem Gebiet Der Rontgenstrahlen Und Der Bildgebenden Verfahren, 2013, 185, 1175-1181.	1.3	7
69	Regorafenib Effects on Human Colon Carcinoma Xenografts Monitored by Dynamic Contrast-Enhanced Computed Tomography with Immunohistochemical Validation. PLoS ONE, 2013, 8, e76009.	2.5	26
70	Perfusion MRI for Monitoring the Effect of Sorafenib on Experimental Prostate Carcinoma: A Validation Study. American Journal of Roentgenology, 2012, 198, 384-391.	2.2	22
71	The Akaike information criterion in DCE-MRI: Does it improve the haemodynamic parameter estimates?. Physics in Medicine and Biology, 2012, 57, 3609-3628.	3.0	21
72	Quantification of Perfusion and Permeability in Multiple Sclerosis. Investigative Radiology, 2012, 47, 252-258.	6.2	86

#	Article	IF	CITATIONS
73	Dynamic Contrast-Enhanced Computed Tomography Imaging Biomarkers Correlated With Immunohistochemistry for Monitoring the Effects of Sorafenib on Experimental Prostate Carcinomas. Investigative Radiology, 2012, 47, 49-57.	6.2	38
74	Comparison of consecutive bolus tracking and flash replenishment measurements for the assessment of tissue hemodynamics using contrast-enhanced ultrasound (CEUS) in an experimental human squamous cell carcinoma model. Clinical Hemorheology and Microcirculation, 2012, 52, 107-114.	1.7	4
75	Contrast agents as a biological marker in magnetic resonance imaging of the liver: conventional and new approaches. Abdominal Imaging, 2012, 37, 164-179.	2.0	25
76	Erratum to "Combined diffusion-weighted and dynamic contrast-enhanced imaging of patients with acute osteoporotic vertebral fractures―[Eur. J. Radiol. 76 (2010) 298–303]. European Journal of Radiology, 2011, 77, 528.	2.6	0
77	Quantitative Pulmonary Perfusion Magnetic Resonance Imaging. Investigative Radiology, 2010, 45, 7-14.	6.2	35
78	Analysis of Signal Dynamics in Oxygen-Enhanced Magnetic Resonance Imaging. Investigative Radiology, 2010, 45, 165-173.	6.2	12
79	Measurement of perfusion and permeability from dynamic contrastâ€enhanced MRI in normal and pathological vertebral bone marrow. Magnetic Resonance in Medicine, 2010, 64, 115-124.	3.0	24
80	MR-perfusion (MRP) and diffusion-weighted imaging (DWI) in prostate cancer: Quantitative and model-based gadobenate dimeglumine MRP parameters in detection of prostate cancer. European Journal of Radiology, 2010, 76, 359-366.	2.6	21
81	Combined diffusion-weighted and dynamic contrast-enhanced imaging of patients with acute osteoporotic vertebral fractures. European Journal of Radiology, 2010, 76, 298-303.	2.6	43
82	Quantification of cerebral blood flow, cerebral blood volume, and blood–brainâ€barrier leakage with DCEâ€MRI. Magnetic Resonance in Medicine, 2009, 62, 205-217.	3.0	225
83	Time-Resolved 3D Pulmonary Perfusion MRI. Investigative Radiology, 2009, 44, 525-531.	6.2	28
84	Influence of multichannel combination, parallel imaging and other reconstruction techniques on MRI noise characteristics. Magnetic Resonance Imaging, 2008, 26, 754-762.	1.8	199